Effect of hydrophobic solutes on the liquid-liquid critical point

Dario Corradini,[1] Sergey V. Buldyrev,[2] Paola Gallo,[1] and H. Eugene Stanley[3]

[1]*Dipartimento di Fisica, Università Roma Tre, Via della Vasca Navale 84, I-00146 Roma, Italy*

[2]*Department of Physics, Yeshiva University, 500 West 185th Street, New York, New York 10033, USA*

[3]*Center for Polymer Studies and Department of Physics, Boston University, Boston, Massachusetts 02215, USA*

Jagla ramp particles, interacting through a ramp potential with two characteristic length scales, are known to show in their bulk phase thermodynamic and dynamic anomalies, similar to what is found in water. Jagla particles also exhibit a line of phase transitions separating a low density liquid phase and a high density liquid phase, terminating in a liquid-liquid critical point in a region of the phase diagram that can be studied by simulations. Employing molecular dynamics computer simulations, we study the thermodynamics and the dynamics of solutions of hard spheres (HS) in a solvent formed by Jagla ramp particles. We consider the cases of HS mole fraction x_{HS}=0.10, 0.15, and 0.20, and also the case x_{HS}=0.50 (a 1:1 mixture of HS and Jagla particles). We find a liquid-liquid critical point, up to the highest HS mole fraction; its position shifts to higher pressures and lower temperatures upon increasing x_{HS}. We also find that the diffusion coefficient anomalies appear to be preserved for all the mole fractions studied.

I. INTRODUCTION

Liquid water exhibits highly unusual thermodynamic and dynamic behavior [1–3]. Among its most known anomalies there are the decrease in density upon isobaric cooling (density anomaly), the apparent divergences of thermodynamic response functions such as the isothermal compressibility, the coefficient of thermal expansion, and the isobaric specific heat upon cooling and the increase in diffusivity upon isothermal compression ("diffusion anomaly"). It has been hypothesized that the thermodynamic anomalies of water may be related to the presence of liquid-liquid (LL) critical point (LLCP) in the deeply supercooled region [4–16]. This hypothesized LLCP is the end point of the liquid-liquid coexistence line separating two distinct liquid phases: a low density liquid (LDL) and a high density liquid (HDL).

Molecular dynamics simulations of water aiming to study the LLCP and phenomena related to it often employ water models that reproduce the tetrahedral orientation-dependent interactions of real water. However several papers have recently shown that tetrahedrality and even orientation-dependent interactions are not necessary conditions for the appearance of the density and the diffusion anomalies or the presence of a LL transition [17–26]. There exists a family of spherically symmetric potentials composed by a hard core and a linear repulsive ramp, the Jagla ramp model [27,28] that can be tuned, varying the ratio between its two characteristic length scales, in order to span the range of behavior from hard spheres to waterlike [24,29,30]. With the appropriate choice of parameters the Jagla ramp potential with two characteristic length scales displays both thermodynamic and dynamic anomalies and a LL transition.

Spherically symmetric potentials with softened core have been used as coarse-grained models for a variety of substances beside water, such as metallic systems and colloidal suspensions [31–33].

Besides its rather unique behavior as a pure liquid, water is also a remarkable solvent. In particular, phenomena related

to the solvation of apolar solutes in water are interesting since they encompass biological membrane formation, globular protein folding, and also the stability of mesoscopic assembly [34–37]. A large number of papers have in the past addressed the phenomenon of hydrophobic hydration (see, for example, Refs. [7,35,38–49]). Small apolar solutes, such as alkanes or noble gases are poorly soluble in water. The solvation free energy of this kind of solutes is large and positive due to the large and negative entropy contribution, the latter having been related to the structure of the hydrophobic hydration shell [48]. These quantities have a marked temperature dependence and one intriguing anomaly of water in solutions is represented by the increase in solubility of hydrophobic gases upon decreasing temperature [50].

Experimentally the solubility of small apolar hydrophobic solutes decreases upon decreasing temperature until a minimum is reached in the temperature range from 310 to 350 K. Upon further temperature decrease, the solubility increase monotonically [34,38]. The solubility of model hydrophobic solutes, hard spheres, in the two-scale ramp potential par-
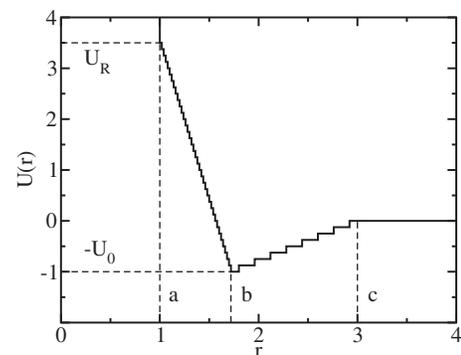

FIG. 1. Spherically symmetric Jagla ramp potential. The potential has two scales: the hard-core diameter $r=a$ and the soft-core diameter $r=b$. In this case U_R/U_0=3.56, b/a=1.72, and c/a=3. We have discretized the potential using a discretization step ΔU =$U_0/8$.
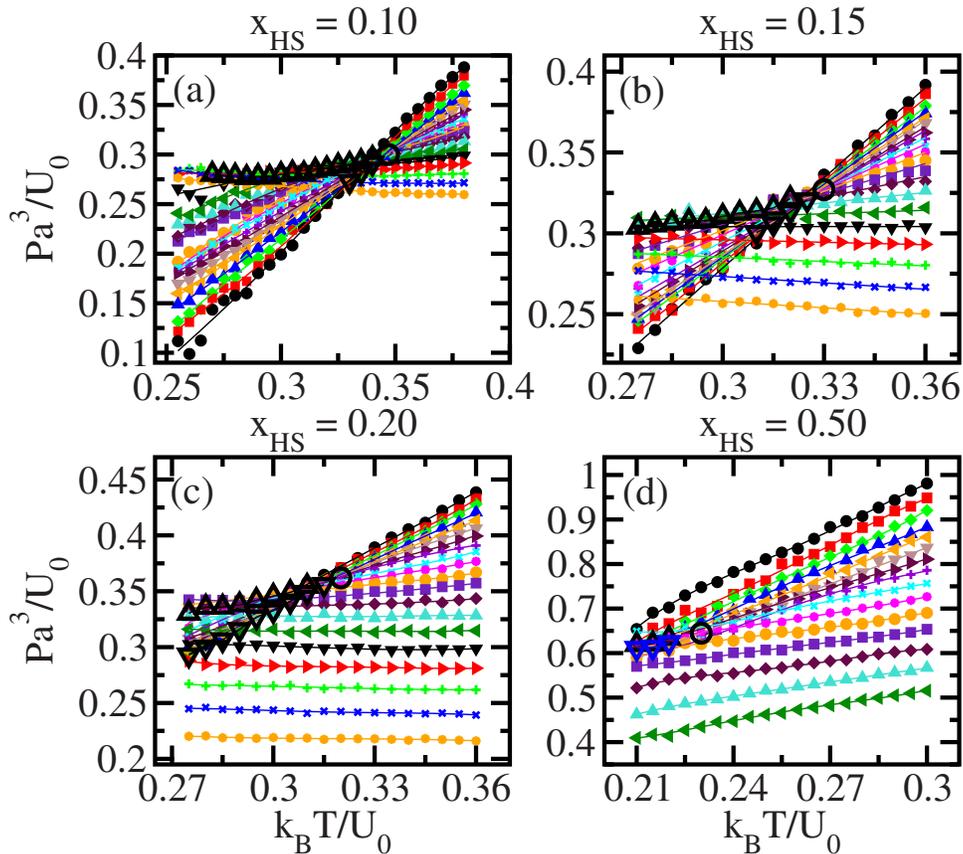
FIG. 2. (Color online) Isochores in the P-T plane for the four solutions at different hard spheres mole fractions. (a) $x_{HS}=0.10$, isochores are drawn for $\rho \equiv Na^3/L^3$ where $L/a=17.4, 17.3, \ldots, 15.5$. The range of corresponding densities span from $\rho=0.328$ to $\rho=0.464$ (from bottom to top). The temperatures range is $0.255 \leq T \leq 0.380$. (b) $x_{HS}=0.15$, isochores are drawn for $\rho \equiv Na^3/L^3$ where $L/a=17.4, 17.3, \ldots, 15.5$. The range of corresponding densities span from $\rho=0.328$ to $\rho=0.464$ (from bottom to top). The temperatures range is $0.275 \leq T \leq 0.360$. (c) $x_{HS}=0.20$, isochores are drawn for $\rho \equiv Na^3/L^3$, where $L/a=17.4, 17.3, \ldots, 15.5$. The range of corresponding densities span from $\rho=0.328$ to $\rho=0.464$ (from bottom to top). The temperatures range is $0.275 \leq T \leq 0.360$. (d) $x_{HS}=0.50$, isochores are drawn for densities $\rho \equiv Na^3/L^3$ where $L/a=15.1, 15, 0, \ldots, 13.7$. The range of corresponding densities span from $\rho=0.502$ to $\rho=0.672$ (from bottom to top). The temperatures range is $0.210 \leq T \leq 0.300$. In all panels the lines are fourth degree polynomial fits to simulated state points. For all mole fractions the position of the LLCP (circles), the LDL LMS (triangles up), and the HDL LMS (triangles down) are also reported.

ticles has been recently assessed [34]. It was found that the mixture of ramp particles and hard spheres shows a temperature of minimum solubility, similarly to experimental results in water. The increased solubility upon cooling is connected to the presence of two repulsive length scales in the model potential, the hard core corresponding to nearest-neighbor shell of solvent molecules and the soft repulsive core. Moreover it was observed that hard spheres are more favorably solvated in low density phases, in accord with what found in simulations of water [7].

The nature of critical phenomena in the presence of solutes has been extensively studied in literature with regard to the liquid-gas critical point [51–53], while the effect of solutes on the LLCP of the solvent is a relatively new subject [54,55].

In this work we investigate the thermodynamic and dynamic properties of the mixture of ramp potential supplemented by an attractive tail and apolar solutes modeled by hard spheres. We examine three mole fractions of hard spheres, $x_{HS}=0.10$, 0.15, and 0.20. We also investigate thermodynamics and diffusivity for a 1:1 mixture of hard spheres

and Jagla ramp particles, $x_{HS}=0.50$. The paper is structured as follows. In Sec. II we give the details of the interaction potential and of the simulation method. We present results and discussion in Sec. III and conclusions in Sec. IV

II. METHODS

We perform discrete molecular dynamics [21,23,56] on systems composed by $N=N_{ramp}+N_{HS}=1728$ particle, where N_{ramp} is the number of waterlike particles and N_{HS} is the number of hard spheres. We study four systems with different composition. The solute content in the four systems is $N_{HS}=173$ for $x_{HS}=0.10$, $N_{HS}=260$ for $x_{HS}=0.15$, $N_{HS}=345$ for $x_{HS}=0.20$, and $N_{HS}=864$ for $x_{HS}=0.50$

The pairwise Jagla ramp interaction potential [27,28] has two characteristic length scales, the hard-core distance $r=a$ and the soft-core distance $r=b$. The minimum of the energy U_0 corresponds to the soft-core distance. An attractive tail extends up to $r=c$. The potential has been discretized, in order to be able to employ the algorithm of discrete molecular dynamics. We partition the repulsive ramp into 36 steps
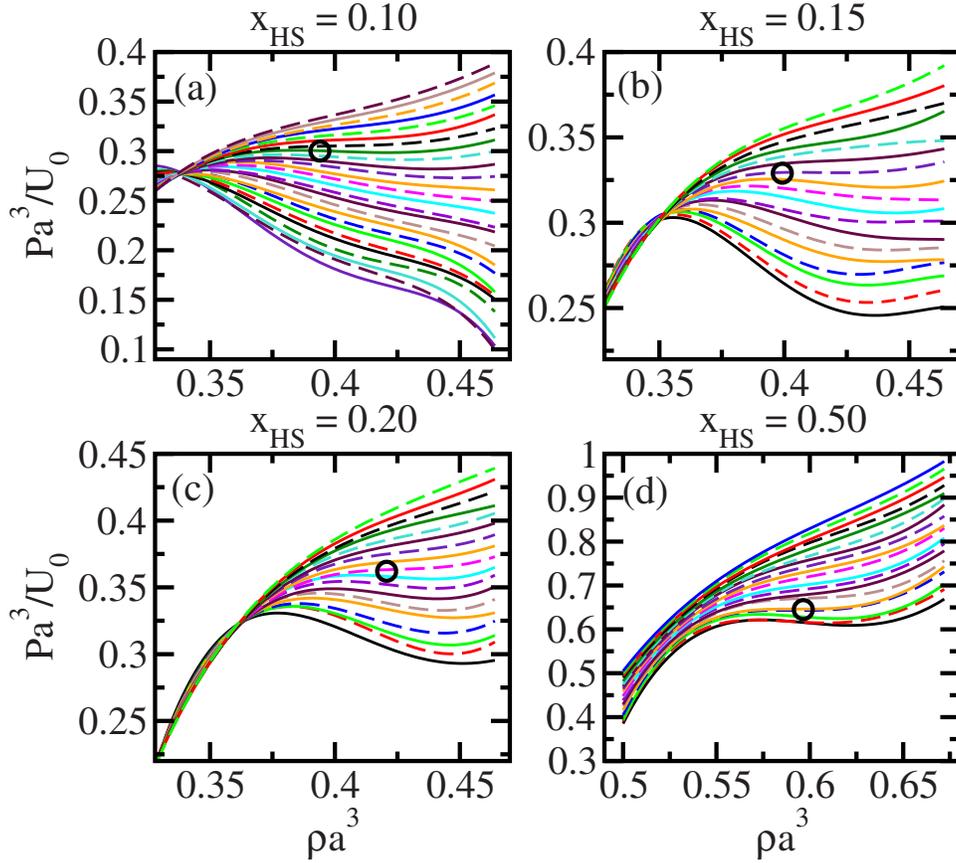
FIG. 3. (Color online) Isotherms in the P-ρ plane for the four solutions at different hard spheres mole fractions. (a) x_{HS}=0.10, isotherms are drawn from T=0.255 to T=0.380 every ΔT=0.005 (from bottom to top). (b) x_{HS}=0.15, isotherms are drawn from T=0.275 to T=0.360 every ΔT=0.005 (from bottom to top). (c) x_{HS}=0.20, isotherms are drawn from T=0.275 to T=0.360 every ΔT=0.005 (from bottom to top). (d) x_{HS}=0.50, isotherms are drawn from T=0.210 to T=0.300 every ΔT=0.005 (from bottom to top). In all panels the lines are fourth degree polynomial fits to simulated state points. The circles represent the position of the LLCP. Every other line has been made dashed to help distinguishing in between them.

of width $0.02a$ and the attractive ramp into eight steps of width $0.16a$. The ΔU at each step is $U_0/8$=0.125. The parameters of the ramp potential [21] have been set to b/a =1.72 and c/a=3. U_R=3.56U_0 is defined as the value of the energy at $r=a$, obtained via least-squares linear fit to the discretized repulsive ramp. The shape of the spherically symmetric Jagla ramp potential employed in this work is shown in Fig. 1. As in previous papers [20,21], this parametrization of the ramp potential prevents the occurrence of crystallization. Furthermore, with this choice of parameters, the line of LL phase coexistence extends into the equilibrium liquid phase and ends in a LLCP. The diameter of the hard spheres is a, the same as the hard-core distance of Jagla ramp interaction potential. The solvent and the solute interact via a hard-core potential.

We express all quantities in reduced units. Distances are in unit of a, energies in units of U_0 and time in units $a\sqrt{m/U_0}$, where m is the mass that is assumed to be unitary. The density defined as $\rho \equiv N/L^3$, where L is the edge of the cubic simulation box, is measured in units of a^{-3}, pressure in unit of U_0/a^3 and temperature in units of U_0/k_B.

We perform simulations at constant N, V, and T, with T controlled by rescaling the velocity of the particles with a modified Berendsen algorithm (details are given in Ref. [56])

or at constant N, P, and T, with P controlled by allowing the edge of the simulation box to vary with time applying the standard Berendsen algorithm [56].

III. RESULTS AND DISCUSSION

We study the thermodynamics of the solutions of hard spheres in Jagla ramp potential waterlike particles, analyzing the isochores in the P-T plane and the isotherms in the P-ρ plane. We study ranges of temperature and density for which the hard spheres are completely soluble in the Jagla ramp potential liquid [34]. As a consequence in the range we study here, no solvent-solute demixing occurs. The position of the LLCP has been estimated considering the inflection point in the isotherms where

$$\left(\frac{\partial P}{\partial \rho}\right)_T = \left(\frac{\partial^2 P}{\partial \rho^2}\right)_T = 0. \tag{1}$$

The points of the LL limit of mechanical stability (LMS) lines have been determined by the points for which $(\partial P/\partial \rho)_T$=0 and $(\partial^2 P/\partial \rho^2)_T \neq 0$ where the isothermal compressibility K_T=$(\partial \rho/\partial P)_T/\rho$ diverges.

The thermodynamic properties of the bulk Jagla ramp potential particles, with the same set of parameters used in this
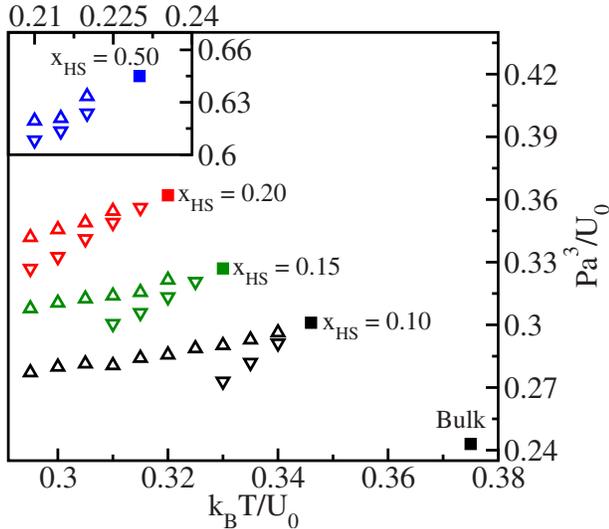
FIG. 4. (Color online) Position in the *P-T* plane of the LLCP (squares) and of LDL (triangles up) and HDL (triangles down) LMS lines for the solutions of hard spheres in Jagla ramp particles, with x_{HS}=0.10, 0.15, and 0.20. The position of the LLCP of bulk Jagla ramp particles is also reported for comparison. In the inset the analogous quantities are shown for the 1:1 mixture of Jagla ramp particles and hard spheres.

TABLE I. Position of the LLCP for bulk Jagla ramp potential particles and for the solutions of hard spheres in Jagla ramp potential particles with x_{HS}=0.10, 0.15, and 0.20 and for 1:1 mixture of Jagla ramp potential particles and hard spheres (x_{HS}=0.50).

x_{HS}	T_c	P_c	ρ_c
0.00 (bulk)	0.375	0.243	0.370
0.10	0.346	0.301	0.394
0.15	0.330	0.327	0.399
0.20	0.320	0.362	0.421
0.50 (1:1 mixture)	0.230	0.645	0.597

work, have been previously assessed [20]. In particular the coordinates in the thermodynamic plane of the LLCP of bulk Jagla ramp potential particles are T_c=0.375, P_c=0.243, and ρ_c=0.37. In Fig. 2 we present the isochores *P-T* plane for all the solutions at different mole fractions. In this figure the location of the LLCP and the two branches of the LL LMS lines are also shown. For mole fractions up to x_{HS}=0.20 we observe that the isochores converge very clearly to the LLCP and cross at points corresponding to the LMS lines. For mole fractions x_{HS}=0.10, 0.15, and 0.20 we also note that the low density isochores appear almost flat, signaling the presence of the density anomaly. The points of the temperature of maximum density line are in fact given by the zeros of the coefficient of thermal expansion, where $(\partial P / \partial T)_\rho$=0. In the case of the mixture with x_{HS}=0.50 the convergence of the isochores to the LLCP appears less precise. In this case we observe that the isochores are not flat any longer, indicating the disappearance of the density anomaly at this high mole fraction of hard spheres.

Figure 3 shows the isotherms of the mixtures with x_{HS}=0.10, 0.15, 0.20, and 0.50 along with the position of the LLCP in the *P-ρ* plane. We can observe the inflection point in the isotherms corresponding to the critical point below which the isotherms show van der Waals-like loops indicating LL coexistence. We also observe that upon increasing the mole fraction of solutes the density range of the region of coexistence narrows. We also point out that for low density the isotherms cross due to density anomaly for mole fractions x_{HS}=0.10, 0.15, and 0.20. In fact for the points where isotherms cross, $(\partial P / \partial T)_\rho$=0, so the crossing of the isotherms indicates a density anomaly. Also in the case of x_{HS}=0.50 mixture the presence of a LLCP can be highlighted by the inflection point in the critical isotherm and the van der

Waals-like loop structure of the isotherms below the critical temperature. An important feature of isotherms of this system is that they do not cross, confirming what we have found looking at the isochores in Fig. 2. For this very high mole fraction of solutes the density anomaly is not longer present, while the LLCP is still found.

The coordinates of the estimated positions of the LLCP for bulk Jagla ramp potential particles [20] and for all the systems with different composition are reported together in Table I.

The positions of the LLCP and the two branches of the LL LMS line for the solutions with x_{HS}=0.10, 0.15, and 0.20 and for the 1:1 system are also reported in Fig. 4 in the *P-T* plane. The position of the LLCP moves to higher pressures and lower temperatures upon increasing the solute mole fraction. This shift of the critical point could be connected to the fact that hard spheres are more favorably solvated in LDL [7,34]. In fact the LDL region of the phase diagram progressively widens upon increasing the mole fraction of hard spheres.

Looking at the isochores (Fig. 2) and at the isotherms (Fig. 3) we can observe that upon increasing the mole fraction of hard spheres, the width of the coexistence envelope is reduced. In fact the region of crossing of the isochores is progressively reduced upon increasing the solute mole fraction, on going from the system at x_{HS}=0.10 to the one at x_{HS}=0.50. Also the width of the loop region in the isotherms plane becomes more narrow spanning a minor range of densities, upon increasing the solute mole fraction. From these considerations we can argue that upon a further increase in solute mole fraction, the LL critical phenomenon will disappear. This is in agreement with studies of the LL transition in aqueous solutions [55,57–59].

In Fig. 5 we present the diffusion coefficients for the Jagla ramp potential particles, calculated at constant temperature as a function of the density of the system, for all the mole fractions studied. For all solute mole fractions, we find the appearance of the diffusivity anomaly. The x_{HS}=0.10, 0.15, and 0.20 mixtures are studied in the same set of densities, ρ=0.328 to ρ=0.464. In this range maxima are evident for x_{HS}=0.10, 0.15, and 0.20, while minima can be seen only for the x_{HS}=0.20 mixture. Minima for the x_{HS}=0.10 and 0.15 mixtures are to be found at lower densities, out of the spanned density range. This is due to the narrowing of the region of the diffusivity anomaly upon increasing the solute mole fraction. Thus not only thermodynamic anomalies but
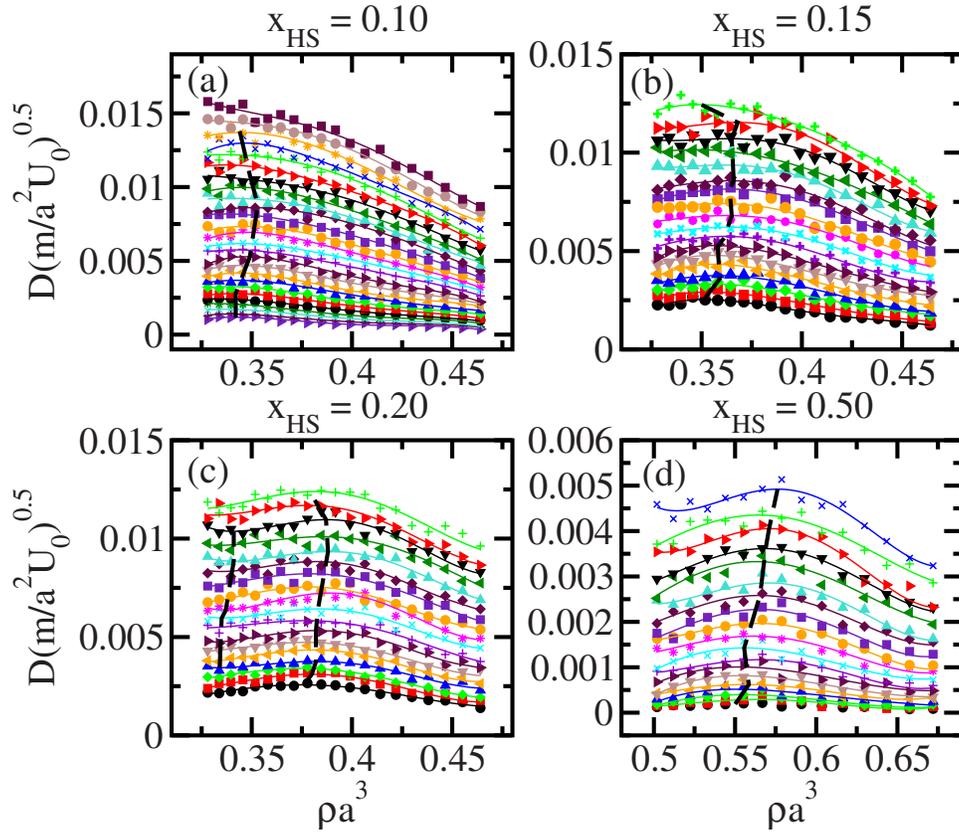
FIG. 5. (Color online) Diffusion coefficients of Jagla ramp particles at constant temperature for the four solutions at different hard spheres mole fractions. (a) $x_{HS}=0.10$, isotherms of the diffusion coefficient are drawn from $T=0.255$ to $T=0.380$ every $\Delta T=0.005$ (from bottom to top). (b) $x_{HS}=0.15$, isotherms of the diffusion coefficient are drawn from $T=0.275$ to $T=0.360$ every $\Delta T=0.005$ (from bottom to top). (c) $x_{HS}=0.20$, isotherms of the diffusion coefficient are drawn from $T=0.275$ to $T=0.360$ every $\Delta T=0.005$ (from bottom to top). (d) $x_{HS}=0.50$, isotherms of the diffusion coefficient are drawn from $T=0.210$ to $T=0.300$ every $\Delta T=0.005$ (from bottom to top). For all panels, the lines are fourth degree polynomial fits to simulated state points. The dashed lines join the diffusivity extrema (maxima for $x_{HS}=0.10, 0.15, 0.50$, maxima and minima for $x_{HS}=0.20$).

also dynamic anomalies exist in a smaller range of densities, upon increasing the solute mole fraction. The diffusion coefficients at constant pressure for the $x_{HS}=0.50$ are studied in the density range $\rho=0.502$ to $\rho=0.672$, thus cannot be directly compared with mixtures with lower solute mole fraction as the range of densities spanned is different. However we can see that they also exhibit diffusion anomaly with the presence of maxima in the isotherms of the diffusion coefficient.

In Fig. 6 we report the behavior of the diffusion coefficient of Jagla ramp particles and hard spheres calculated for a constant pressure path above the critical pressure for the solutions with hard sphere mole fractions $x_{HS}=0.10$, 0.15, and 0.20. For all compositions the pressure is set to the critical pressure plus $\Delta P=0.020$. In the bulk Jagla ramp particles system it was found that the trend of the diffusion coefficient, calculated on a cooling path above the critical point, shows a crossover from a high-temperature behavior (LDL-like) to a stronger (HDL-like) behavior [20]. This change in trend was connected to the maximum of the specific heat that occurs at the Widom line via the Adam-Gibbs equation $D=D_0 \exp(-C/TS_{conf})$, where S_{conf} is the configurational entropy. We can observe that the crossover in the behavior of the diffusion coefficient is maintained up to the highest mole
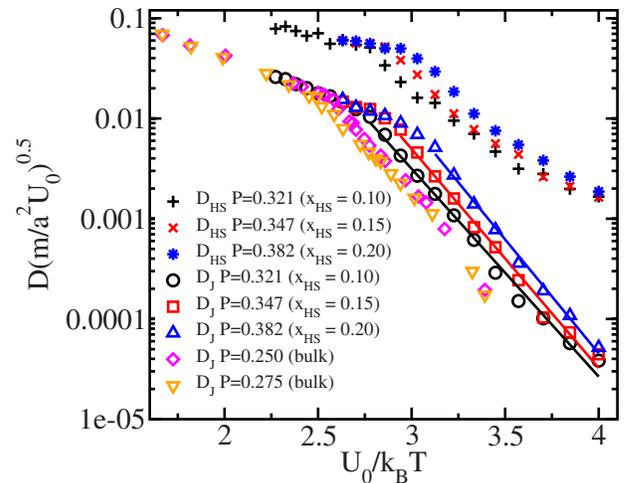

FIG. 6. (Color online) Diffusion coefficients for hard spheres and Jagla ramp particles along a constant pressure path above the critical point. $P=0.321$ for $x_{HS}=0.10$, $P=0.347$ for $x_{HS}=0.15$ and $P=0.382$ for $x_{HS}=0.20$. Lines correspond to the Arrhenius fit for the Jagla ramp particles. In this figure the diffusion coefficients at constant pressure for the bulk Jagla ramp particles at $P=0.250$ and $P=0.275$ are also reported for comparison.
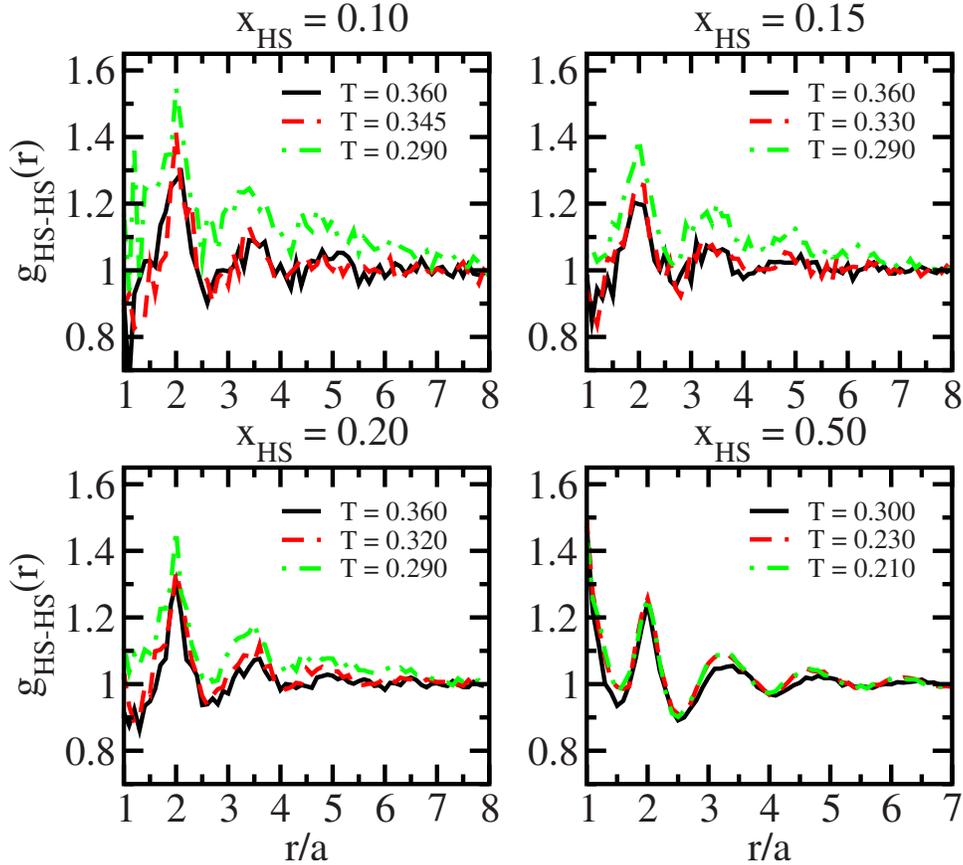
FIG. 7. (Color online) Hard sphere–hard sphere radial distribution functions for the mixtures with x_{HS}=0.10, 0.15, 0.20, and 0.50 calculated at their critical densities (see Table I). The $g_{HS-HS}(r)$ are reported at temperatures T=0.360, 0.345, and 0.290 for x_{HS}=0.10, T=0.360, 0.330, and 0.290 for x_{HS}=0.15, T=0.360, 0.320, and 0.290 for x_{HS}=0.15, and T=0.300, 0.230, and 0.210 for x_{HS}=0.50.

fraction studied (x_{HS}=0.20), and at low enough temperature, below the Widom line, for all compositions the diffusion behavior becomes that of a HDL Jagla liquid. The temperature at which the dynamic crossover occurs decreases upon increasing the mole fraction of solutes. As the Widom line is connected to the LLCP, the shift to lower temperatures of the dynamic crossover confirms the shift to lower temperatures of the LLCP we have found studying the thermodynamics (see Fig. 4). The trend of the diffusion coefficient of hard spheres closely follows that of the Jagla ramp potential particles, thus we can derive that the diffusive behavior of the hard spheres solute is determined by the solvent.

Therefore we conclude that the dynamic crossover found in bulk Jagla ramp particles system (analogous to liquid water) at the Widom line, is preserved in the solutions and that the temperature of dynamic crossover decreases, upon increasing the mole fraction of hydrophobic solutes.

Finally the solute-solute radial distribution functions are shown in Fig. 7. The $g_{HS-HS}(r)$ have been reported for the critical density of the systems and for three temperatures, T=0.360, the critical temperature and T=0.290 for the solutions with x_{HS}=0.10, 0.15, and 0.20 and for T=0.300, the critical temperature and T=0.210 for x_{HS}=0.50. A small tendency of the solutes to cluster upon increasing concentration can be seen looking at the progressive increase in the $g(r)$ near the hard-core distance. At the lowest temperature the

solute-solute radial distribution functions also show anomalous behavior with a progressive decay toward the asymptotic value of 1 at large r that tends to disappear upon increasing the mole fraction of solutes. The decay indicates segregation of the HS into the LDL phase below the critical point.

IV. CONCLUSIONS

We performed discrete molecular dynamics simulations on the mixture of Jagla ramp potential (waterlike) particles and hard spheres, at four different compositions, x_{HS}=0.10, 0.15, 0.20, and 0.50. The thermodynamic and dynamic behavior were studied for the solutions with x_{HS}=0.10, 0.15, and 0.20. Thermodynamics and diffusive behavior were also studied for the 1:1 mixture of Jagla ramp particles and hard spheres.

The analysis of the isochores and the isotherms plane revealed the presence of a liquid-liquid critical point for all the investigated system. We also found that while density anomaly is present in the solutions with x_{HS}=0.10, 0.15, and 0.20, it disappears for the 1:1 mixture. Furthermore we also observe a narrowing of the coexistence envelope in both planes, upon increasing the solute mole fraction. The position of the critical point is found to shift toward lower temperatures and higher pressures, upon increasing the hard

sphere mole fraction. This shift may be related to the favored solvation of hard spheres in the LDL Jagla ramp potential particles solvent.

The complete phase diagram of the solution in the vicinity of the LLCP may be quite complex and might include also an upper critical solution temperature different from the LLCP. The interplay of these two critical points is an interesting subject which deserves separate investigation.

The appearance of extrema in the behavior of the constant temperature diffusion coefficient for Jagla ramp potential particles, i.e., the diffusion anomaly is also preserved up to the highest mole fraction of hard spheres studied, with a narrowing of the anomalous region upon increasing the solute mole fraction, also for this dynamic property.

Finally a change in trend of the constant pressure diffusion coefficient from LDL-like behavior to HDL-like behavior can be observed when cooling the system in a constant pressure path, above the critical pressure. This crossover in the dynamic behavior can be related to the crossing of the Widom line, above the critical point. The dynamic crossover observed for bulk Jagla ramp particles at the Widom line shifts to lower temperatures upon increasing the content of solutes.

[1] P. G. Debenedetti, J. Phys.: Condens. Matter **15**, R1669 (2003) and references therein.

[2] P. G. Debenedetti and H. E. Stanley, Phys. Today **56**(6), 40 (2003).

[3] J. R. Errington and P. G. Debenedetti, Nature (London) **409**, 318 (2001).

[4] P. H. Poole, F. Sciortino, U. Essman, and H. E. Stanley, Nature (London) **360**, 324 (1992).

[5] P. H. Poole, I. Saika-Voivod, and F. Sciortino, J. Phys.: Condens. Matter **17**, L431 (2005).

[6] P. H. Poole, F. Sciortino, T. Grande, H. E. Stanley, and C. A. Angell, Phys. Rev. Lett. **73**, 1632 (1994).

[7] D. Paschek, Phys. Rev. Lett. **94**, 217802 (2005).

[8] D. Paschek, A. Rüppert, and A. Geiger, ChemPhysChem **9**, 2737 (2008).

[9] H. Tanaka, J. Chem. Phys. **105**, 5099 (1996).

[10] I. Brovchenko, A. Geiger, and A. Oleinikova, J. Chem. Phys. **123**, 044515 (2005).

[11] P. Jedlovszky and R. Vallauri, J. Chem. Phys. **122**, 081101 (2005).

[12] M. Yamada, S. Mossa, H. E. Stanley, and F. Sciortino, Phys. Rev. Lett. **88**, 195701 (2002).

[13] F. Sciortino, P. H. Poole, U. Essmann, and H. E. Stanley, Phys. Rev. E **55**, 727 (1997).

[14] F. Sciortino, E. La Nave, and P. Tartaglia, Phys. Rev. Lett. **91**, 155701 (2003).

[15] O. Mishima and H. E. Stanley, Nature **392**, 164 (1998); **396**, 329 (1998).

[16] S. Harrington, P. H. Poole, F. Sciortino, and H. E. Stanley, J. Chem. Phys. **107**, 7443 (1997).

[17] M. Canpolat, F. W. Starr, M. R. Sadr-Lahijany, A. Scala, O. Mishima, S. Havlin, and H. E. Stanley, Chem. Phys. Lett. **294**, 9 (1998).

[18] M. R. Sadr-Lahijany, A. Scala, S. V. Buldyrev, and H. E. Stanley, Phys. Rev. Lett. **81**, 4895 (1998).

[19] L. Xu, P. Kumar, S. V. Buldyrev, S.-H. Chen, P. H. Poole, F. Sciortino, and H. E. Stanley, Proc. Natl. Acad. Sci. U.S.A. **102**, 16558 (2005).

[20] L. Xu, S. V. Buldyrev, C. A. Angell, and H. E. Stanley, Phys. Rev. E **74**, 031108 (2006).

[21] L. Xu, S. V. Buldyrev, N. Giovambattista, C. A. Angell, and H. E. Stanley, J. Chem. Phys. **130**, 054505 (2009).

[22] L. Xu, I. Ehrenberg, S. V. Buldyrev and H. E. Stanley, J. Phys.: Condens. Matter **18**, S2239 (2006).

[23] P. Kumar, S. V. Buldyrev, F. Sciortino, E. Zaccarelli, and H. E. Stanley, Phys. Rev. E **72**, 021501 (2005).

[24] Z. Yan, S. V. Buldyrev, N. Giovambattista, and H. E. Stanley, Phys. Rev. Lett. **95**, 130604 (2005).

[25] H. M. Gibson and N. B. Wilding, Phys. Rev. E **73**, 061507 (2006).

[26] E. Lomba, N. G. Almarza, C. Martin, and C. McBride, J. Chem. Phys. **126**, 244510 (2007).

[27] E. A. Jagla, Phys. Rev. E **58**, 1478 (1998).

[28] E. A. Jagla, J. Chem. Phys. **111**, 8980 (1999).

[29] Z. Yan, S. V. Buldyrev, N. Giovambattista, P. G. Debenedetti, and H. E. Stanley, Phys. Rev. E **73**, 051204 (2006).

[30] Z. Yan, S. V. Buldyrev, P. Kumar, N. Giovambattista, and H. E. Stanley, Phys. Rev. E **77**, 042201 (2008).

[31] J. Fornleitner and G. Kahl, EPL **82**, 18001 (2008).

[32] G. Malescio and G. Pellicane, Phys. Rev. E **70**, 021202 (2004).

[33] S. V. Buldyrev, G. Malescio, C. A. Angell, N. Giovambattista, S. Prestipino, F. Saija, H. E. Stanley, and L. Xu, J. Phys.: Condens. Matter **21**, 504106 (2009).

[34] S. V. Buldyrev, P. Kumar, P. G. Debenedetti, P. J. Rossky, and H. E. Stanley, Proc. Natl. Acad. Sci. U.S.A. **104**, 20177 (2007).

[35] K. Lum, D. Chandler, and J. D. Weeks, J. Phys. Chem. B **103**, 4570 (1999).

[36] C. Tanford, *The Hydrophobic Effect: Formation of Micelles and Biological Membranes*, 2nd ed. (Wiley, New York, 1980).

[37] W. Kauzmann, Adv. Protein Chem. **14**, 1 (1959).

[38] H. S. Ashbaugh, T. M. Truskett, and P. G. Debenedetti, J. Chem. Phys. **116**, 2907 (2002).

[39] H. S. Ashbaugh, S. Garde, G. Hummer, E. W. Kaler, and M. E. Paulatis, Biophys. J. **77**, 645 (1999).

[40] H. S. Ashbaugh and L. R. Pratt, Rev. Mod. Phys. **78**, 159 (2006).

[41] F. H. Stillinger, J. Solution Chem. **2**, 141 (1973).

[42] L. R. Pratt and D. Chandler, J. Chem. Phys. **67**, 3683 (1977).

[43] L. R. Pratt, Annu. Rev. Phys. Chem. **53**, 409 (2002).

[44] S. Garde, G. Hummer, A. E. Garcia, M. E. Paulaitis, and L. R. Pratt, Phys. Rev. Lett. **77**, 4966 (1996).

[45] G. Hummer, S. Garde, A. E. Garcia, A. Pohorille, and L. R. Pratt, Proc. Natl. Acad. Sci. U.S.A. **93**, 8951 (1996).

[46] G. Hummer, S. Garde, A. E. Garcia, M. E. Paulatis, and L. R. Pratt, J. Phys. Chem. B **102**, 10469 (1998).

[47] S. Rajamani, T. M. Truskett, and S. Garde, Proc. Natl. Acad. Sci. U.S.A. **102**, 9475 (2005).

[48] B. Widom, P. Bhimalapuram, and K. Koga, Phys. Chem. Chem. Phys. **5**, 3085 (2003).

[49] J. Holzmann, R. Ludwig, A. Geiger, and D. Paschek, ChemPhysChem **9**, 2722 (2008).

[50] E. Wilhelm, R. Battino, and R. J. Wilcox, Chem. Rev. **77**, 219 (1977).

[51] P. H. Van Konynenburg and R. L. Scott, Philos. Trans. R. Soc. London, Ser. A **298**, 495 (1980).

[52] R. L. Scott and P. H. van Konynenburg, Discuss. Faraday Soc. **49**, 87 (1970).

[53] A. I. Abdulagatov, G. V. Stepanov, and I. M. Abdulagatov, Therm. Eng. **55**, 706 (2008); **55**, 795 (2008).

[54] S. Chatterjee and P. G. Debenedetti, J. Chem. Phys. **124**, 154503 (2006).

[55] D. Corradini, M. Rovere, and P. Gallo, J. Chem. Phys. **132**, 134508 (2010).

[56] S. V. Buldyrev, in *Aspects of Physical Biology*, Lecture Notes in Physics, edited by G. Franzese and M. Rubi (Springer-Verlag, Berlin, 2008), p. 97.

[57] D. G. Archer and R. W. Carter, J. Phys. Chem. B **104**, 8563 (2000).

[58] D. Corradini, P. Gallo, and M. Rovere, J. Chem. Phys. **128**, 244508 (2008).

[59] D. Corradini, P. Gallo, and M. Rovere, J. Chem. Phys. **130**, 154511 (2009).